ACS APPLIED MATERIALS & INTERFACES

Research Article

www.acsami.org

Independent Control of Adhesive and Bulk Properties of Hybrid Silica Coatings on Polycarbonate

Krystelle Lionti,[†] Linying Cui,[‡] Willi Volksen,[†] Reinhold Dauskardt,*[,‡] Geraud Dubois,*[,†,‡] and Berangere Toury*[,§]

[†]IBM Almaden Research Center, San Jose, California 95120, United States

[‡]Department of Materials Science and Engineering, Stanford University, Stanford, California 94305-4034, United States

[§]Laboratoire des Multimateriaux et Interfaces, UMR 5615, University of Lyon, Villeurbanne, 69622, France

ABSTRACT: Transparent polymers are widely used in many applications ranging from automotive windows to microelectronics packaging. However, their intrinsic characteristics, in particular their mechanical properties, are significantly degraded with exposure to different weather conditions. For instance, under humid environment or UV-irradiation, polycarbonate (PC) undergoes depolymerization, leading to the release of Bisphenol A, a molecule presumed to be a hormonal disruptor, potentially causing health problems. This is a serious concern and the new REACH (**R**egistration, **E**valuation, **A**uthorization and Restriction of **Ch**emical substances) program dictates that materials releasing Bisphenol A should be removed from the market by January 1st, 2015 (2012-1442 law). Manufacturers have tried to satisfy this new regulation by depositing atop the PC a dense oxide-like protective coating that would act as a barrier layer. While high hardness, modulus, and density can be achieved by this approach, these coatings suffer from poor adhesion to the PC as evidenced by the numerous delamination events occurring under low scratch constraints. Here, we show that the combination of a N_2/H_2-plasma treatment of PC before depositing a hybrid organic-inorganic solution leads to a coating displaying elevated hardness, modulus, and density, along with a very high adherence to PC (> 20 J/m^2 as measured by double cantilever beam test). In this study, the sol-gel coatings were composed of hybrid O/I silica (based on organoalkoxysilanes and colloidal silica) and designed to favor covalent bonding between the hybrid network and the surface treated PC, hence increasing the contribution of the plastic deformation from the substrate. Interestingly, double-cantilever beam (DCB) tests showed that the coating's adhesion to PC was the same irrespective of the organoalkoxysilanes/colloidal silica ratio. The versatility of the sol-gel deposition techniques (dip-coating, spray-coating, etc.), together with the excellent mechanical properties and exceptional adherence of this hybrid material to PC should lead to interesting new applications in diverse fields: optical eye-glasses, medical materials, packaging, and so forth.

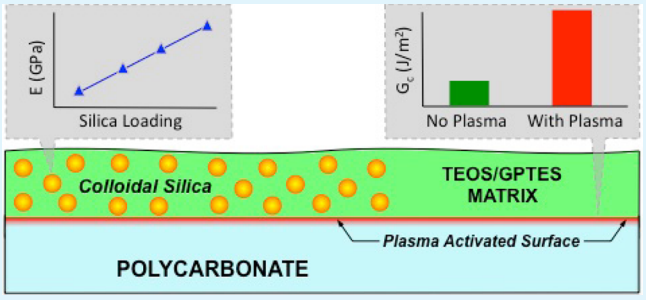

KEYWORDS: *polycarbonate, sol-gel, hybrid silica, elastic properties, adhesion, plasma treatment, double cantilever beam*

INTRODUCTION

Polycarbonate (PC) is widely used commercially because of its interesting characteristics such as transparency, lightness, high impact resistance, along with an excellent quality/price ratio. However, PC suffers from low scratch resistance and poor stability in humid environment or UV exposure, leading to a decrease in the material's lifetime and to the release of Bisphenol A, a molecule highly suspected to be detrimental for human health. As of today, two different approaches have been mainly considered to mitigate these issues: formulating PC-based copolymers,[1] or modifying the PC surface with a protective coating.[2−6] While the latter approach is more challenging, it provides a very attractive solution to the industry if the adhesion, the bulk mechanical properties, and the barrier properties of such coatings could be precisely controlled. Therefore, the research in this field has mainly focused on the optimization of the coating's bulk mechanical properties. In this regard, hybrid organic/inorganic silica coatings prepared by sol-gel chemistry have received lots of attention because of the possibility to enhance the mechanical properties through the inorganic part while imparting other specific properties for a given application with the organic functionalities.[7] The sol-gel route also presents several other advantages such as, the availability of a large library of precursors, implementability with low cost equipment, and compatibility with PC's relatively low glass transition temperature (143 °C).

In this paper, highly transparent hybrid silica coatings issued from 3-glycidoxypropyltriethoxysilane (GPTES), tetraethylorthosilicate (TEOS), and colloidal silica prepared by the sol-gel

Received: August 20, 2013
Accepted: October 2, 2013
Published: October 2, 2013

route under acidic conditions and dip-coated on untreated and plasma pretreated PC are reported. This selection of precursors should ensure good mechanical properties for the bulk due to the silica network[8,9] as well as an elevated interfacial fracture energy if plastic deformation within the PC could be activated. The effect of the precursor's ratio and the PC pretreatment on the bulk hardness, Young's modulus, and density, along with the adhesive fracture energy are thus investigated. As expected, both the hardness and the elastic modulus measured using nanoindentation and the density measured by X-ray reflectivity increased with increasing inorganic content, that is, colloidal silica. The coatings adhesive fracture energy (G_c) was quantified by a double cantilever beam (DCB) test, a newly adapted technique for polymeric substrates. To the best of our knowledge, it has never been reported for sol-gel hybrid silica films deposited on PC. The G_c values increased from less than 2 J/m^2 to more than 20 J/m^2 when the PC surface was pretreated with a nitrogen based plasma. Moreover, the excellent film adhesive properties are maintained over long time storage as the same G_c values were obtained after aging for 1 year under atmospheric conditions. Surprisingly, the coatings fracture energy was not affected when the colloidal silica content varied from 10 to 50 wt %. Altogether, these results demonstrate that the bulk and the adhesive properties of such hybrid coatings can be independently controlled. It could be envisioned that with the proper pretreatment, precursors selection and sol-gel conditions, tunable optical, electrical, mechanical, and surface properties could be achieved while preserving the interfacial integrity of the coating to the polymeric substrate.

EXPERIMENTAL METHODS

Coating Preparation. Coatings were prepared by the sol-gel route using TEOS and GPTES as alkoxysilanes and commercially available colloidal silica (Levasil 200E from AKZONOBEL, with an average particles size of 30 nm). Solutions with different alkoxysilanes/colloidal silica weight ratios ranging from 50/50 to 90/10 have been prepared. The coating deposition was realized after 36 h of sol aging by dip-coating at 1 mm/s, on both untreated and pretreated PC. Regarding the latter, a N_2/H_2 plasma treatment was performed by AcXys Technologies company (atmospheric pressure, 300 mm/s flow rate) on the PC surface prior to coating deposition. Atomic force microscopy (AFM) analysis performed after treatment did not indicate any change in terms of surface roughness. Finally, the coated samples were annealed under air in a ventilated oven at 135 °C for 1 h. Several micrometer-thick coatings were obtained. The coating preparation steps and deposition are fully described in reference 8.

Characterization. The density, ρ, of the coating was measured by specular X-ray reflectivity (XRR) using a diffractometer (X'Pert Pro MRD, Panalytical, Westborough, MA) with a ceramic X-ray tube (λ = 0.154 nm) and high resolution horizontal goniometer (reproducibility = ± 0.0001°). The critical angle, θ_c, from the reflectivity data was obtained from the peak position of $I \times q^4$ versus q plot, where I is the reflected X-ray intensity, $q = (4p/\lambda) \times \sin\theta$, λ is the wavelength, and θ is the grazing angle of the X-ray beam. The coating density ρ was inferred from the electronic density ρ_e calculated using the equation

$$\rho_e = \frac{\theta_c}{\lambda} \times \frac{\pi}{r_e} \times \frac{A}{Z} \times N_A$$

where r_e is the classical electron radius, A the atomic mass number, Z the atomic number, and N_A the Avogadro number.

Quasi-static nanoindentation measurements were performed on a commercial nanoindenter, Hysitron Model TI-950, with a diamond cube corner (three-sided pyramid) probe of 40 nm end radius. To eliminate adsorbed moisture that could complicate measurements of mechanical properties, nanoindentation was carried out under a positive pressure of dry nitrogen in the closed indenter enclosure. Freshly loaded samples were allowed to equilibrate with dry nitrogen for at least 12 h that also allows for thermal equilibrium. The cube corner probe was calibrated on a quartz sample with a modulus of 70 GPa. As the probe was indenting the sample, both contact depth (h) and applied load (P) were monitored. Seven different loads ranging from 7 μN to 25 μN with 7 runs per load were carried out on each sample. At the maximum indentation depth, the load was kept constant for 5 sec. A load versus contact depth curve was then generated from the collected data. The reduced Young's modulus E_r and hardness H were further calculated based on their relationship with the contact area A_c and the sample stiffness S using the following equations:

$$H = \frac{P_{max}}{A_c}$$

$$E_r = \frac{1}{\beta}\frac{\sqrt{\pi}}{2} \times \frac{S}{\sqrt{A_c}}$$

The effective contact area A_c was calculated from the contact depth and the tip geometry using the Oliver and Pharr method.[10] The stiffness was obtained from the slope of the unloading curve $(\partial P)/(\partial h)$.

The Young's modulus, E_f, was then calculated from the reduced modulus E_r, taking into account elastic displacements from both the film and the indenter, using the equation

$$\frac{1}{E_r} = \frac{(1-\nu_i^2)}{E_i} + \frac{(1-\nu_f^2)}{E_f}$$

where E_i is the indenter Young's modulus (1140 GPa), ν_i the indenter poisson's ratio (0.07), and ν_f the film poisson's ratio (assigned as 0.25).

The coatings adhesion energy on PC was quantified using the symmetric Double Cantilever Beam (DCB) test. The specimens were prepared by bonding a blank (uncoated) substrate of 2 mm- thickness onto a coated substrate of the same thickness. The in-plane dimensions of the specimen were 9 mm × 70 mm. The fracture tests were conducted on a micromechanical adhesion test system (DTS Delaminator Test System, DTS Company, Menlo Park, CA) in displacement control mode. The specimens were loaded at a displacement rate of 5 μm/sec in tension to produce controlled crack growth, followed by unloading. The load was measured simultaneously and the adhesion energy G_c (J/m^2) was calculated from the critical value of the strain energy release rate using the Kanninen corrected equation[11]

$$G_c = \frac{12 \times P_c^2}{E \times B^2 \times h} \times \left(\frac{a}{h} + 0.64\right)^2$$

where P_c is the load when the load−displacement curve deviated from linearity until initial crack extension, E the plane strain Young's modulus of the substrate, B the substrate width, a the crack length, and h the substrate thickness.

X-ray photoelectron spectroscopy (XPS) [Physical Electronics Inc, Chanhassen, MN] was used to characterize the atomic composition of the DCB fracture surfaces throughout the bulk. An Al−Kα (1486 eV) X-ray source with a spot size of ∼1 mm was used in conjunction with an argon ion beam to sputter off the material at a rate of 4 nm/min for the silica coatings, with the setting of 1 kV, 0.5 μA, and 1 mm × 1 mm sputter spot. The angle between the detector and the sample surface was 45°. The scan range for the binding energy was 0 to 1000 eV.

RESULTS AND DISCUSSION

Four different sol-gel solutions with alkoxysilanes/colloidal silica weight ratios of 50/50, 70/30, 80/20, and 90/10 were studied. The alkoxysilanes contribution comes from a mixture of GPTES and TEOS with a constant TEOS/GPTES molar ratio of 1.65. Regarding the coatings' thermal treatment, the low annealing temperature of the samples (set at 135 °C to stay below the T_g of PC) should prevent the formation of highly

densified silica. Therefore, pre-condensed colloidal silica was added to the solutions to strengthen the final coating. As described previously,[8] sol-gel solutions were aged for 36 h before deposition, to ensure completion of the hydrolysis reaction while condensation is still at an early stage.[12] This should lead to maximum bonding between the coating and the substrate during film deposition and curing.

To assure the substrate's integrity over time, it was highly important to assess the coatings bulk properties with regards to raw PC, and also to evaluate the coatings' adhesion to the substrate, a critical component of the coating's lifetime. Those two characteristics were studied separately. The bulk mechanical properties (Young's modulus and hardness) and density were measured by nanoindentation, and by X-ray reflectivity, respectively. The coatings fracture energy was obtained from symmetric DCB tests.

Bulk Properties. First, we measured the coatings densities by X-ray reflectivity as a function of the colloidal silica content (Figure 1). In the range of 10 to 50 wt % colloidal silica, the

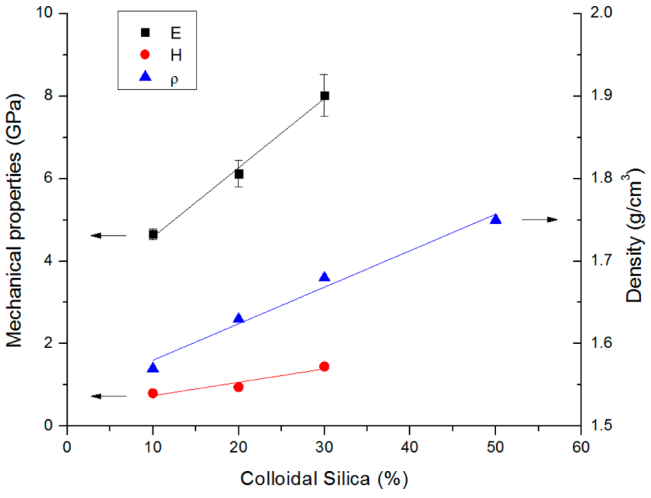

Figure 1. Coatings Young's modulus (E), hardness (H), and density (ρ) as a function of colloidal silica percentage as measured by nanoindentation. Hardness standard deviation was always smaller than 0.1 GPa and is not represented here. Pure silica Young's modulus hardness and density from literature respectively are 72 GPa, 8 GPa, and 2.2 g/cm^3.

density increased linearly from 1.57 g/cm^3 to 1.75 g/cm^3. As expected, the addition of pre-densified silica nanoparticles leads to a significant change in film bulk properties. Interestingly, by extrapolating the density data to 100 wt % colloidal silica, one would obtain a density of 1.94 g/cm^3, a value close to the one of dense silica coatings (2.2 g/cm^3) deposited by gas phase deposition techniques.[13] The results above indicate that the intrinsic density of the nanoparticles is around 1.94 g/cm^3 and that they are well dispersed throughout the main bulk of the film. Moreover, the absence of porosity, as indicated by ellipsometric measurements,[8] suggests that the intimate mixing of the nanoparticles within the hybrid network was successfully achieved.

Next, nanoindentation experiments were conducted on the different coatings to study the influence of the silica nanoparticle loading on the bulk Young's modulus and hardness (Figure 1). The contact depth measured at the different loads for coatings with up to 30 wt % silica nanoparticles was always smaller than a tenth of the total film thickness (2−3 μm), minimizing the substrate effect.[14] Conversely, nanoindentation data indicated a strong substrate contribution for 50 wt % colloidal silica content coatings, because of the lower film thickness (1.2 μm) combined with the substrate plasticity and consequently they are not reported here. Both Young's modulus and hardness were found to increase when the colloidal silica percentage was varied from 10 to 30 wt %. The Young's modulus almost doubled, increasing from 4.7 GPa to 8.0 GPa while the hardness changed by more than 80 %, from 0.8 GPa to 1.5 GPa. In comparison, the Young's modulus and hardness of PC are respectively 2.5 GPa and 0.17 GPa.[15] These data clearly demonstrate the mechanical benefits obtained by depositing such coatings onto PC. These values are also similar to the ones reported for silica particle doped sol-gel coatings on different substrates. Depending upon both the silica particle content and the alkoxysilanes nature, moduli between 1 and 15 GPa and hardness of 0.2 to 2 GPa have been obtained by nanoindentation.[2,3,16−21] Altogether, this confirms that the addition of pre-densified silica enables the toughening of a broad range of organosilicate films. Moreover, the linear increase of the film mechanical properties is in good agreement with the one observed for the density over the same colloidal silica range. These results support that the silica nanoparticles are homogeneously distributed within the hybrid network. Finally, it demonstrates that such a toughening strategy can be applied when low thermal requirements need to be satisfied.

Film/PC Interfacial Adhesion. The adhesive fracture energy (G_c) of the various coatings was obtained by symmetric DCB. This technique specifically measures the adhesion between a coating and a substrate independently of any other mechanical characteristics. This is fundamentally different from the scratch test technique where the samples are stressed both normally and tangentially at the same time. In this case, the lower force at which cracking occurs (Lc1) is a function of both bulk mechanical properties and interfacial adhesion. Nevertheless, this technique has been widely utilized for the qualitative characterization of protective coatings on PC.[9,19,22] Conversely, DCB was only recently adapted to polymeric substrates,[11,23] permitting quantitative measurements of the adhesive fracture energy. Coatings with different composition deposited both on untreated and N_2/H_2 plasma pretreated PC were studied. The G_c values measured on untreated and plasma treated PC as a function of composition are plotted in Figure 2.

All coatings display similar behavior: the plasma treatment leads to a significant increase in G_c from 1−2 J/m^2 to more than 20 J/m^2, and the adhesion of the sol-gel film to the substrate is unaffected by the colloidal silica loading. It is worth noting that the fracture occurred at the hybrid film to PC interface as indicated by the X-ray photoelectron spectroscopy (XPS) surface analysis results shown in Figure 3. The low interfacial fracture energy measured for the pristine PC is not surprising as the hydrophilic coating should have little interaction with the hydrophobic PC surface. In this case, adhesive debonding occurs at low applied stress at the interface and consequently little energy can be dissipated in the PC substrate. After the plasma treatment the PC surface becomes hydrophilic, that is, the water contact angle drops from 82° to less than 40°. The formation of polar bonds, such as, C−OH and C-NH_2 has already been evidenced by XPS,[8] it not only renders the PC surface more hydrophilic but it also most likely leads to covalent bonding with both organic and inorganic moieties from the hybrid network.[24] The interaction between

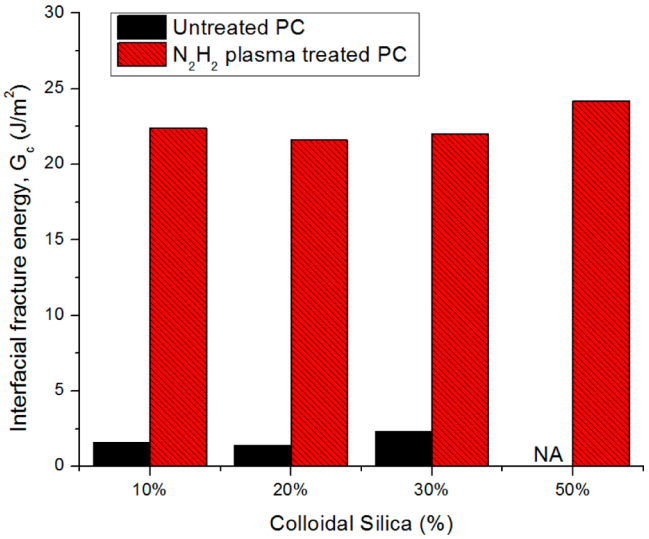

Figure 2. Coatings adhesive fracture energy as a function of colloidal silica ratio on untreated or N_2/H_2 plasma treated PC as measured by DCB.

the hybrid coating and the PC is therefore increased. Furthermore, plasma treatments are known to roughen the polymer surface creating a larger contact surface between the two materials.[25,26] These two factors are responsible for the 10 fold increase in interfacial fracture energy after plasma treatment: the higher energy input required to overcome the stronger interaction between the coating and the substrate results in a higher stress state at the vicinity of the crack tip, and more energy is dissipated in the substrate and coating because of plastic deformation. While the plasma treatment time was not optimized for this specific coating, it is unlikely that a low molecular weight layer (LMWL) due to PC over-exposure was formed in our case. Indeed, the presence of a LMWL on PC leads to a rapid decay of the adhesive fracture energy with G_c values <10 J/m^2 for silica coatings deposited by atmospheric plasma.[11]

The colloidal silica content seems to have little or no effect on the adhesion to PC. While surprising at first, this can be rationalized if there is no segregation of silica nanoparticles at the interface and if the plastic properties of the hybrid network do not significantly change. It has been shown in the case of polymeric nanoparticles that segregation at the substrate interface occurs with hydrophilic surfaces and is a function of the nanoparticles' loading.[27] We believe that the use of a water based sol-gel solution minimizes this segregation phenomenon as all the hydrolyzed silicate species will maintain strong interaction with the Si−OH surface covered silica nanoparticles after film deposition. This is in good agreement with the XRR and nanoindentation data, which indicated a homogeneous composition throughout the film thickness. XPS depth profiling analysis of the beams after G_c measurement confirmed that the fracture occurred at the film to PC interface and that its composition was identical to the bulk. An example of such profile is shown in Figure 3 for the 30 wt % loading colloidal silica sample. Despite the high carbon content initially detected (coming from both atmospheric contamination and polymeric residues after fracture) and removed with 30 sec of sputtering, the concentration of carbon, silicon, and oxygen atoms is constant from the fractured interface into the bulk.

Regarding plastic deformation of the hybrid network, it can only be influenced by the GPTES amount if polymeric chains are formed through epoxide opening.[28] Even at 10 wt % colloidal silica loading (i.e. maximum GPTES content), the low G_c value measured on untreated PC indicates that there is little or no hybrid network plastic deformation. In this case, increasing the stiffness of the hybrid network with the addition of more silica nanoparticles would certainly not add plasticity to

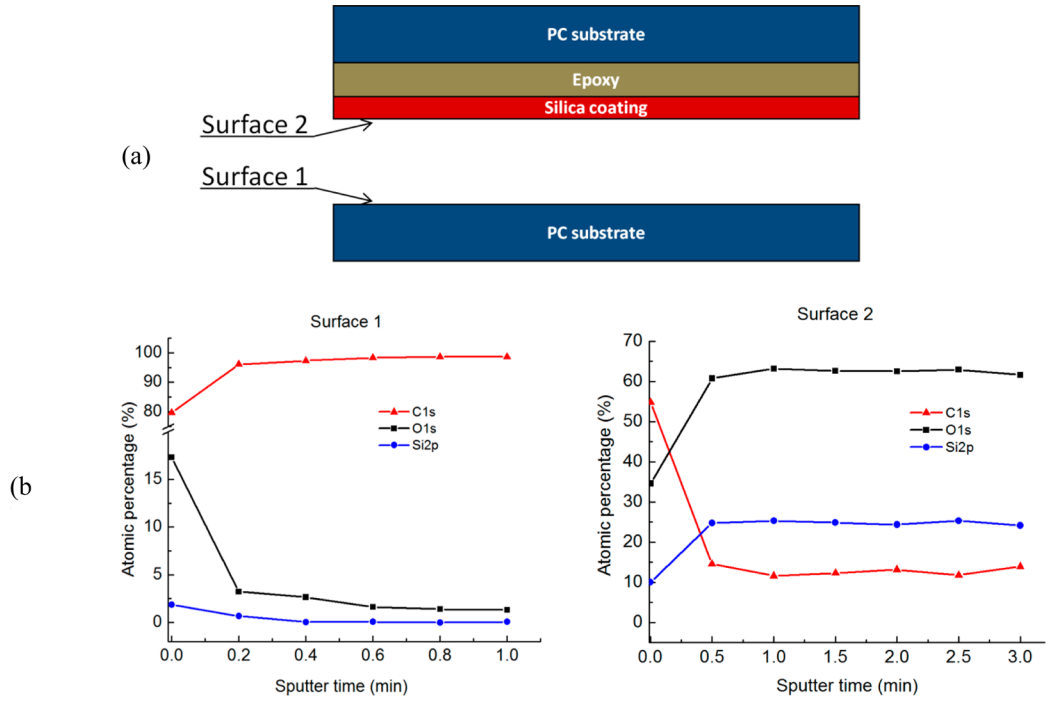

Figure 3. (a) Scheme of ideal XPS analyzed surfaces (after DCB fracture) and (b) XPS depth profile of the interfacial layer between the PC substrate (surface 1) and the 30 wt % loading colloidal silica coating (surface 2).

the coating. Conversely, for plasma treated PC, the high G_c values measured indicate that plastic deformation has been activated in both the PC substrate and the hybrid network. However, the lack of change in G_c values when decreasing the coating organic content suggests that the contribution of the hybrid network plastic deformation is minimal compared to that in PC.

Finally, 10, 20, and 30 wt % colloidal silica loading samples were prepared the same day but their interfacial fracture energy was measured after 1 year interval to probe the robustness of the film towards environmental conditions. The results presented in Table 1 demonstrate that the interfacial fracture energy is not affected by the coating aging time. Consequently, these sol-gel hybrid films could be potential candidates for development toward industrial applications.

Table 1. Interfacial Fracture Energy Measured in the Wake of Coating Deposition (Test 1) and after Aging for 1 Year (Test 2)

	G_c (J/m^2)	
colloidal silica %	test 1	test 2
10 wt %	24.9 ± 2.1	19.8 ±2.9
20 wt %	20.2 ± 2.1	23.0 ±2.4
30 wt %	20.1 ± 2.8	23.9 ±2.5

CONCLUSION

In conclusion, we have demonstrated that the bulk properties and the interfacial adhesion of PC protective coatings based on sol-gel chemistry can be independently controlled. The use of pre-condensed silica nanoparticles to toughen the hybrid network while respecting the thermal requirements due to the low glass transition temperature of the PC substrate was successfully achieved. DCB was used for the first time to quantitatively measure the interfacial fracture energy of sol-gel hybrid silica films deposited on PC. For these films, the adhesion was only a function of the PC plasma surface pretreatment and independent of the silica content. With nanoparticle loadings ranging from 30 to 50 wt %, the Young's modulus was >8.0 GPa and the adhesive fracture energy G_c was found to be >20 J/m^2. These values remained unchanged after aging at ambient conditions for 1 year, making this protective coating very attractive for further development. The protective coating mechanical properties are currently under investigation under environmental conditions known to degrade PC: UV exposure and high humidity. If the correlation between these properties and PC degradation can be established, it might provide a novel way to assess BPA release in applications where PC toxicity is a concern.

AUTHOR INFORMATION

Corresponding Authors

*E-mail: dauskardt@stanford.edu (R.H.D.).
*E-mail: toury@univ-lyon1.fr (B.T.).
*E-mail: gdubois@us.ibm.com (G.D.).

Notes

The authors declare no competing financial interest.

ABBREVIATIONS

PC, polycarbonate; O/I, organic/inorganic; DCB, double-cantilever beam; GPTES, 3-glycidoxypropyltriethoxysilane; TEOS, tetraethylorthosilicate; XRR, X-ray reflectivity; XPS, X-ray photoelectron spectroscopy; Tg, glass transition temperature; LMWL, low molecular weight layer

REFERENCES

(1) Fabbri, P.; Leonelli, C.; Messori, M.; Pilati, F.; Toselli, M.; Veronesi, P.; Morlat-Therias, S.; Rivaton, A.; Gardette, J. L. *J. Appl. Polym. Sci.* **2008**, *108*, 1426−1436.
(2) Wouters, M. E. L.; Wolfs, D. P.; van der Linde, M. C.; Hovens, J. H. P.; Tinnemans, A. H. A. *Prog. Org. Coat.* **2004**, *51*, 312−320.
(3) Soloukhin, V. A.; Posthumus, W.; Brokken-Zijp, J. C. M.; Loos, J.; de With, G. *Polymer* **2002**, *43*, 6169−6181.
(4) Keranen, M.; Gnyba, M.; Raerinne, P.; Kololuoma, T.; Maaninen, A.; Rantala, J. T. *J. Sol-Gel Sci. Technol.* **2004**, *31*, 369−372.
(5) Su, C. H.; Lin, C. R.; Chang, C. Y.; Hung, H. C.; Lin, T. Y. *Thin Solid Films* **2006**, *498*, 220−223.
(6) Li, C. H.; Wilkes, G. L. *J. Inorg. Organomet. Polym.* **1997**, *7*, 203−216.
(7) Sanchez, C.; Julian, B.; Belleville, P.; Popall, M. *J. Mater. Chem.* **2005**, *15*, 3559−3592.
(8) Lionti, K.; Toury, B.; Boissière, C.; Benayoun, S.; Miele, P. *J. Sol-Gel Sci. Technol.* **2013**, *65*, 52−60.
(9) Wu, L. Y. L.; Chwa, E.; Chen, Z.; Zeng, X. T. *Thin Solid Films* **2008**, *516*, 1056−1062.
(10) Oliver, W. C.; Pharr, G. M. *J. Mater. Res.* **1992**, *7*, 1564−1583.
(11) Cui, L.; Ranade, A. N.; Matos, M. A.; Pingree, L. S.; Frot, T. J.; Dubois, G.; Dauskardt, R. H. *ACS Appl. Mater. Interfaces* **2012**, *4*, 6587−6598.
(12) Livage, J.; Sanchez, C. *J. Non-Cryst. Solids* **1992**, *145*, 11−19.
(13) Volksen, W.; Miller, R. D.; Dubois, G. *Chem. Rev.* **2010**, *110*, 56−110.
(14) Veprek, S.; Veprek-Heijman, M. G. J.; Karvankova, P.; Prochazka, J. *Thin Solid Films* **2005**, *476*, 1−29.
(15) Benitez, F.; Martinez, E.; Galan, M.; Serrat, J.; Esteve, J. *Surf. Coat. Technol.* **2000**, *125*, 383−387.
(16) Zheng, C.; Lin, A. m.; Zhen, X.; Feng, M.; Huang, J.; Zhan, H. *Opt. Mater.* **2007**, *29*, 1543−1547.
(17) Chen, Z.; Wu, L. Y. L.; Chwa, E.; Tham, O. *Mater. Sci. Eng., A* **2008**, *493*, 292−298.
(18) Robertson, M. A.; Rudkin, R. A.; Parsonage, D.; Atkinson, A. *J. Sol-Gel Sci. Technol.* **2003**, *26*, 291−295.
(19) Han, Y.-H.; Taylor, A.; Knowles, K. M. *Surf. Coat. Technol.* **2009**, *203*, 2871−2877.
(20) Etienne, P.; Sempere, R. *Verre* **1998**, *4*, 2−10.
(21) Ferchichi, A.; Calas-Etienne, S.; Smaihi, M.; Etienne, P. *J. Non-Cryst. Solids* **2008**, *354*, 712−716.
(22) Hwang, D. K.; Moon, J. H.; Shul, Y. G.; Jung, K. T.; Kim, D. H.; Lee, D. W. *J. Sol-Gel Sci. Technol.* **2003**, *26*, 783−787.
(23) Kamer, A.; Larson-Smith, K.; Pingree, L. S. C.; Dauskardt, R. H. *Thin Solid Films* **2011**, *519*, 1907−1913.
(24) Innocenzi, P.; Kidchob, T.; Yoko, T. *J. Sol-Gel Sci. Technol.* **2005**, *35*, 225−235.
(25) Gonzalez, E. I.; Hicks, R. F. *Langmuir* **2010**, *26*, 3710−3719.
(26) Tang, S.; Choi, H. S. *J. Phys. Chem. C* **2008**, *112*, 4712−4718.
(27) Ong, M. D.; Volksen, W.; Dubois, G.; Lee, V.; Brock, P. J.; Deline, V. R.; Miller, R. D.; Dauskardt, R. H. *Adv. Mater.* **2008**, *20*, 3159−3164.
(28) Brusatin, G.; Innocenzi, P.; Guglielmi, M.; Babonneau, F. *J. Sol-Gel Sci. Technol.* **2003**, *26*, 303−306.